9th AUSTRALASIAN
FLUID MECHANICS CONFERENCE,
AUCKLAND, 8-12 DECEMBER 1986

Flow Measurements in a High Pressure Ratio Thrust Augmenting Ejector

S. A. FISHER and A. M. ABDEL-FATTAH

Aeronautical Research Laboratories, Defence Science and Technology Organisation, Australia.

ABSTRACT

Pressure probing coupled with flow visualisation was used to gain insight into the entrainment mechanisms occurring in an ejector duct with primary jet stagnation pressures up to 50 atmospheres. Variations in ejector thrust were matched by changes in the flow structure, involving unsteady phenomena which might be exploited to enhance mixing in certain specialised ejector applications.

NOMENCLATURE

D_e	Ejector duct diameter
L_e	Ejector length measured from nozzle exit plane
M	Mach number
P	Static pressure
P_a	Atmospheric pressure
P_{o1}	Primary nozzle stagnation pressure
x	Axial distance downstream from nozzle exit plane
y	Radial distance inwards from duct wall.

INTRODUCTION

Aerodynamic ejectors are useful in a variety of pumping and flow augmentation applications, in combustion systems, and for thrust augmentation of jets for low speed propulsion. In the past, attention has generally been focussed on ejectors with primary jet velocities extending only into the low supersonic range, for purposes such as exhaust cooling systems for jet engine test cells and thrust augmentors for VSTOL aircraft. In recent years there has also been interest in the performance of ejectors with jets of much higher velocity such as the efflux from rocket motors and solid propellant gas generators, there being potential for application of the technology to thrust augmentation of hovering rocket vehicles and fuel/air mixing in ramrocket combustion systems.

The performance of axisymmetric thrust augmenting ejectors has been explored with primary jet stagnation pressures as high as 50 atmospheres, using both unheated air jets and solid propellant rocket motors (Fisher, 1980, Fisher and Irvine, 1981, Irvine, 1983). The main purpose was to determine the effect of a wide range of geometric and primary flow parameters on the level of thrust augmentation available. In the course of these investigations, pressure probing and flow visualisation was used to explore the mixing flow in an ejector duct with an unheated air jet, paying particular attention to the effect of certain naturally occurring unsteady flow phenomena on the entrainment process. The present paper presents some of the results of these experiments.

APPARATUS

The test rig is illustrated schematically in Figure 1, which also shows the model geometry. The ejector configuration chosen for these experiments was a simple one, in which the primary jet was directed axially into the bellmouth inlet of a cylindrical duct through a convergent-divergent nozzle with a conical expansion. The nozzle expansion ratio was 4.03 and the nozzle exit, whose diameter was one sixth of the duct diameter, was positioned in the plane of the bellmouth throat. Some thrust results will be presented for a number of values of ejector length L_e, but all of the flow measurement results which follow relate to one non-dimensional length, L_e/D_e = 4.25.

The ejector duct, which had a diameter D_e = 111 mm, was mounted on a force balance with its axis horizontal, independently from the primary nozzle. The primary air was delivered from storage vessels via a control valve, at pressures up to 5 MPa and at room temperature.

Wall static pressure tappings were distributed along the length of the duct, and access was provided for a traversing pitot/static probe at various axial locations. Pressures were recorded using both digital data acquisition equipment and, in the case of signals from the traversing probe, analogue X-Y recorders.

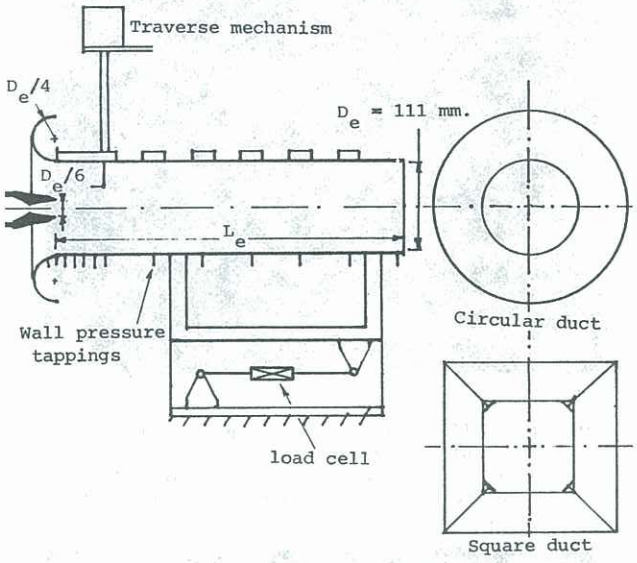

Figure 1 : Schematic diagram of the ejector test rig

For schlieren flow visualisation a duct of square cross section with corner fillets was used, as shown in Figure 1,to gain optical access through plane transparencies. The cross sectional area and length of this duct were equal to those of the axisymmetric duct which it was meant to simulate.

THRUST CHARACTERISTICS

The axial thrust on ejector ducts of various length, measured with no probe in the flow, varied with primary jet pressure ratio as shown in Figure 2. Included for comparison is a theoretical curve based on conservation of mass, momentum and energy. The theoretical assumptions include zero friction at the duct walls and fully mixed (one-dimensional) flow at the exit, so this curve is independent of duct length. These two assumptions, made in the absence of a reliable model of the mixing flow in the ejector, are the main reason for the difference between the theoretical and experimental results. The experimental curve for each value of L_e/D_e generally featured a thrust peak in the range P_{o1}/P_a = 16 to 18, coincident with the occurrence of discrete tones in the

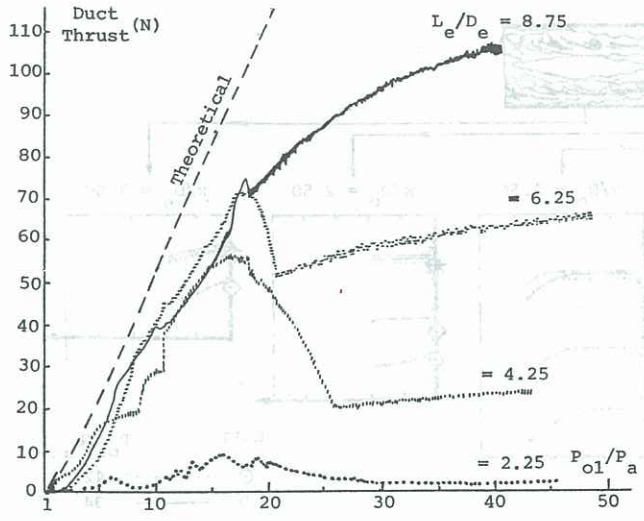

Figure 2 : Duct thrust characteristics for a family of ejectors with different L_e/D_e ratio

emitted noise which indicated acoustic resonance in the ejector duct. The upper boundary of the pressure range in which resonance occurred, which generally coincided with a sharp change in the slope of the thrust characteristic, varied with ejector geometry; for L_e/D_e = 4.25, for example, it occurred at about P_{o1}/P_a = 26. The thrust maxima were most pronounced with intermediate duct lengths and, except for the shortest duct tested, approximated the highest thrust which could have been obtained at the same primary pressure ratio by increasing duct length. This suggested that the flow at the ejector exit had been rendered more or less uniformly mixed by duct resonance, the remaining difference between the experimental and theoretical thrust levels being mainly due to friction effects.

The flow measurements described in the following sections were carried out to identify, in terms of mean flow parameters, the changes in the ejector flow associated with these phenomena. The measurements were confined to the L_e/D_e = 4.25 geometry (this having exhibited the most pronounced thrust peak due to resonance) and concentrated on the range of P_{o1}/P_a extending to the right of the thrust peak in Figure 2.

DUCT STATIC PRESSURES

Figure 3 shows how the wall mean static pressure measured at various streamwise locations in the ejector duct varied with primary jet pressure ratio. The shape of each curve was generally related to the thrust characteristic for L_e/D_e in Figure 2, featuring a distinct change in slope at about P_{o1}/P_a = 26 and a minimum near P_{o1}/P_a = 18. This relationship exists because the internal static pressure (especially at the upstream end - x/D_e = 0, for example) is directly related to the level of entrainment or, taking another viewpoint, to the bellmouth wall suction pressures which represent the sole source of ejector thrust.

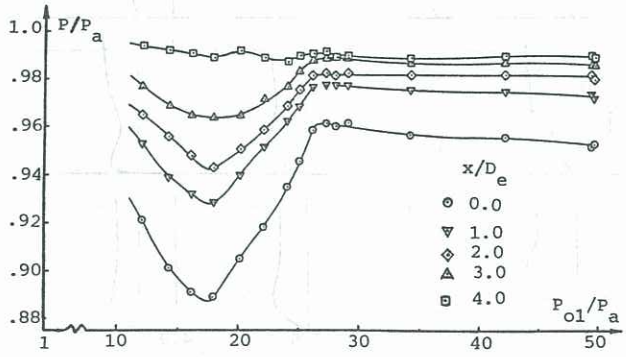

Figure 3 : Variation of wall mean static pressure with P_{o1}/P_a, for different x/D_e

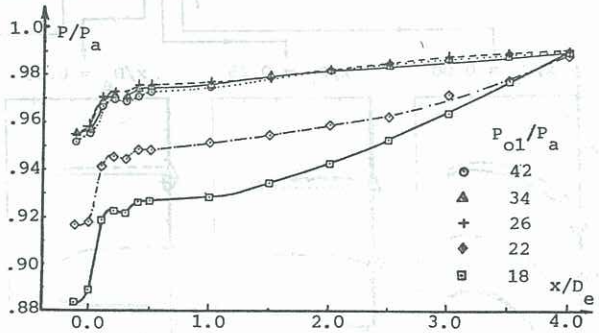

Figure 4 : Streamwise Variation of wall mean static pressure for different P_{o1}/P_a

In Figure 4 the streamwise distribution of wall static pressure is shown for a number of values of primary pressure ratio. The curves for P_{o1}/P_a = 22 and 18 both exhibited increased pressure gradients over the downstream part of the duct, evidently associated with more rapid mixing due to duct resonance; at peak thrust (P_{o1}/P_a = 18) the enhanced gradient appeared downstream of approximately x/D_e = 1.2. The steep gradients in the bellmouth region were associated with the surface velocity distribution around the curved lip, and the irregularity in each curve in the range x/D_e = 0.15 to 0.4 suggested the existence of a separation bubble in that region.

A conventional subsonic pitot/static probe 1.6 mm in diameter was used to traverse the outer part of the flow at each measuring station, to obtain profiles of local mean static pressure. The inner part of the flow (the jet core) was generally supersonic with imbedded shock cells; any attempt to probe this region, besides presenting problems in terms of aerodynamic loads on the probe, would not have yielded useful static pressure results. Indeed, all of the pressure probe results had to be interpreted with care because of the possible influence of probe intrusion on the flow being measured. This effect was monitored by means of wall static pressures and is not thought to have had a significant bearing on the results presented here.

Figure 5 shows radial profiles of mean static pressure measured at a number of streamwise locations, for the same set of primary jet pressure ratios as was used in Figure 4. Corresponding wall static pressures are included; these were reasonably consistent with the radial profiles, with some noticeable exceptions at P_{o1}/P_a = 18 and 22; ie during duct resonance. The flow at this condition tended to be unstable and difficult to reproduce precisely. The effect of probe intrusion may also have contributed. In addition to the expected radial variation of static pressure due to streamline curvature in the bellmouth region (x/D_e = 0), there was a common tendency for the pressure to decrease as the boundary of the jet core was approached from the wall. This effect, evidently associated with the entrainment process, is consistent with observations elsewhere (Quinn et al, 1985). It highlights the risk in frequently made assumptions of uniform static pressure across non-uniform flows.

The streamwise variation of local mean static pressure at different distances from the duct wall appears in Figure 6, for P_{o1}/P_a = 26 (just outside the boundary of duct resonance) and P_{o1}/P_a = 18 (peak thrust). The shapes of the curves in the bellmouth throat region are all consistent with the existence of a separation bubble at the wall.

VELOCITY DISTRIBUTIONS

A more robust pitot probe was used for complete radial traverses of the flow, to determine mean velocity profiles. This involved measurement of pitot pressures which generally varied over a very large range, requiring the use of a number of transducers of different sensitivity, and composite

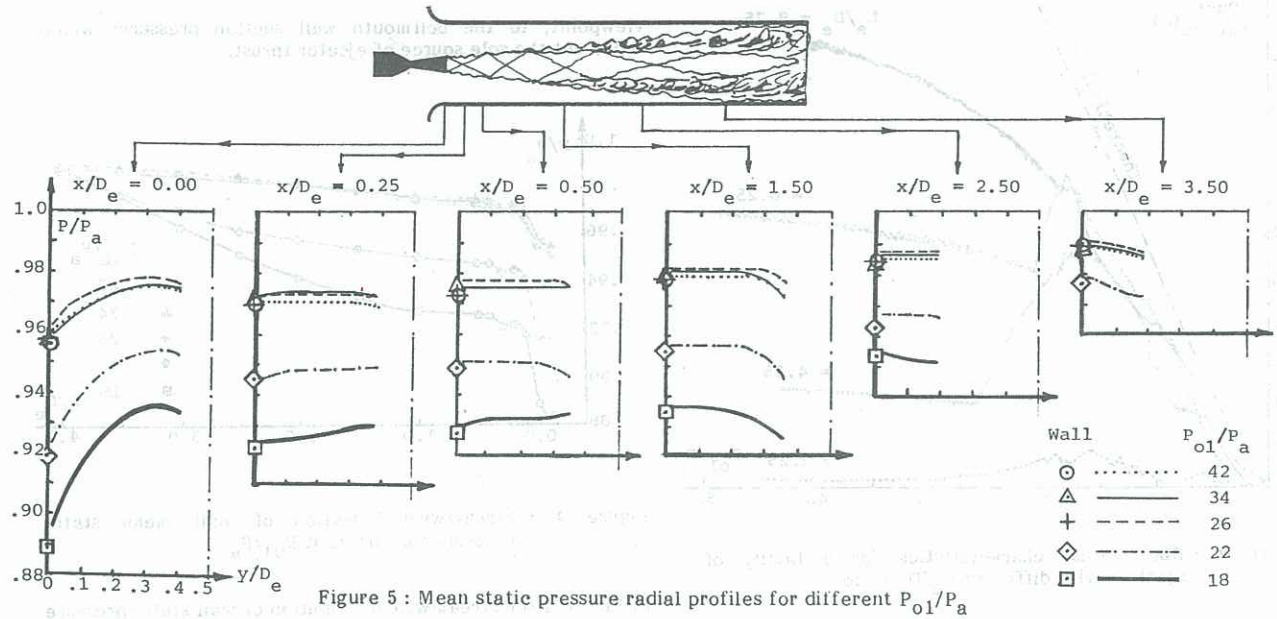

Figure 5 : Mean static pressure radial profiles for different P_{o1}/P_a

construction of profiles. For reasons outlined in the previous section, complete radial profiles of static pressure were not available. Notwithstanding foregoing remarks concerning radial non-uniformity of static pressure, mean Mach number profiles were therefore calculated using local pitot pressure and the relevant wall static. In parts of the flow such as the supersonic jet core, there would have been significant differences between the local static pressure and the adjacent wall pressure, so the profiles are known to be not entirely genuine; they do nevertheless convey valuable information concerning entrainment and jet spread characteristics.

A set of such Mach number profiles is presented in Figure 7 for each of four different values of primary jet pressure ratio. Results for $P_{o1}/P_a = 16$ are included for reasons which will become clear later. The position of the primary nozzle exit lip is represented on each set of profiles for reference. Comments relating to some notable features in Figure 7 are:

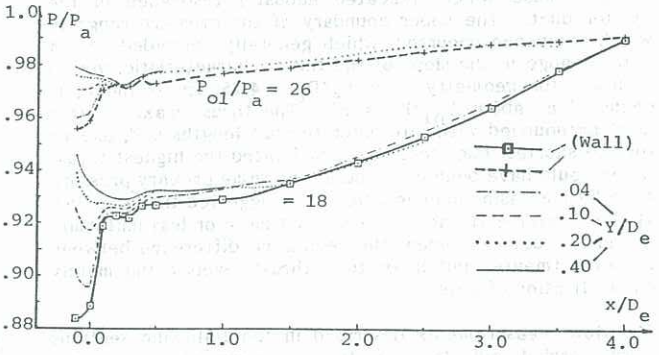

Figure 6 : Streamwise variation of local mean static pressure at different distances from the duct wall

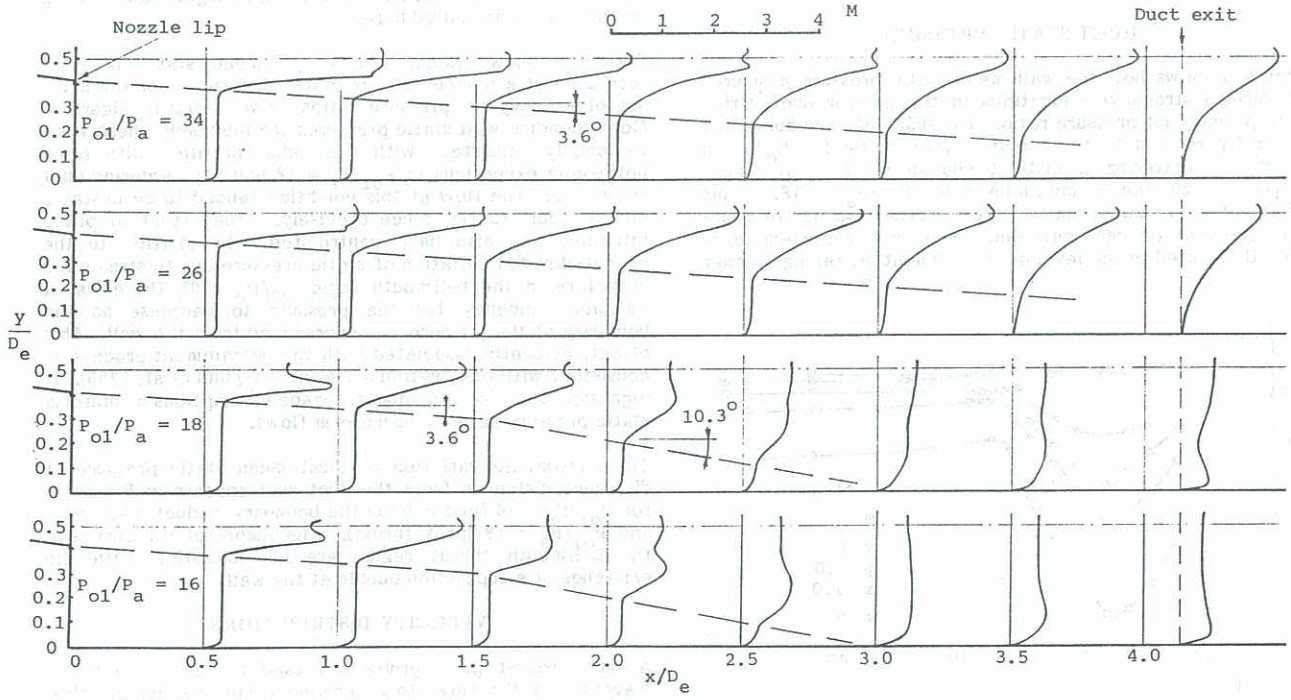

Figure 7 : Mean Mach number profiles calculated from local pitot pressure and wall static pressure

(a) Irregularly shaped profiles evident in the upstream part of the jet core are thought to be related to the shock cell structure.

(b) At the two non-resonant flow conditions included (P_{o1}/P_a = 34 and 26), where random turbulent mixing is presumed to have been the main entrainment mechanism, the jet core remained identifiable at the duct exit. At P_{o1}/P_a = 26, the lowest pressure ratio at which non-resonant flow existed, the calculated peak Mach number at the exit was still about 1.5.

(c) A well defined "edge" of the spreading jet, matched to the nozzle exit lip position, revealed a mean spread half-angle of 3.6° for non-resonant flows, independent of primary jet pressure ratio. For resonant flow conditions the same spread angle appeared to exist upstream of about x/D_e = 1.5, but downstream of that location the angle increased almost threefold.

(d) Duct resonance appeared to result in an annular area of high energy flow (in mean velocity terms), first evident at about x/D_e = 1.5, which increased rapidly in diameter with downstream development. This was finally manifested in a peak in the mean velocity profile adjacent to the duct wall, and an overall profile shape at the duct exit which was highly beneficial to the entrainment rate and duct thrust. The phenomenon described is most clearly evident in the set of profiles for P_{o1}/P_a = 16.

FLOW VISUALISATION

The resonance characteristics of the plane walled duct used for schlieren observation were somewhat more complex than those of the "equivalent" axisymmetric ejector. Nevertheless, it is believed that the flow phenomena involved were similar, such that schlieren photography using the plane walled duct provided reliable qualitative information on the nature of the flow in the axisymmetric case.

Figure 8 contains short exposure photographs of part of the mixing flow taken at two levels of primary jet pressure ratio,

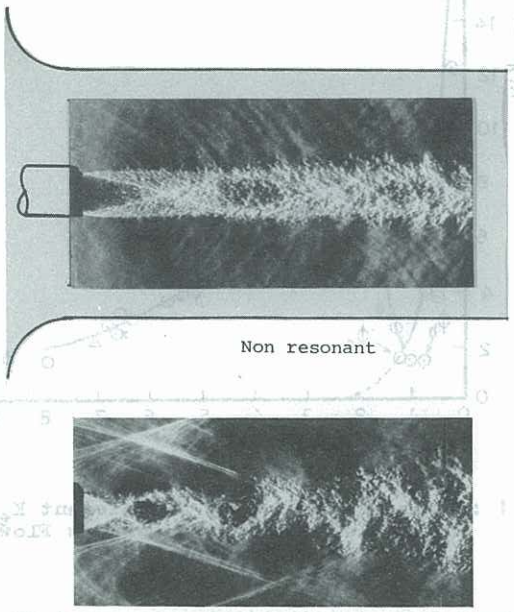

Figure 8 : Schlieren Pictures of the axisymmetric jet in the square duct during relatively stable and resonant flow conditions

one outside the upper boundary of duct resonance and the other at peak resonance. These conditions occurred at pressure ratios which were different from those relating to the corresponding conditions in the axisymmetric configuration, emphasising the qualitative nature of the analogy between the differently shaped ducts. In interpreting the photographs it should be remembered that bands of flow adjacent to the upper and lower surface were obscured by corner fillets. At the resonant condition the jet appeared to adopt a helical instability, evidently driven by pressure waves reflected from the duct walls. Once the unstable flow had developed, the effective spread rate of the jet increased markedly.

DISCUSSION

The present paper provides inadequate space for detailed analysis and description of the observed flows. Further in-depth study of the resonance phenomenon (Abdel-Fattah, 1985) is well advanced and will be reported in full in due course. Superficially, the resonant flow evidently involved helical instability of the jet, with interspersed helical vortices, such that the distribution of axial mean velocity over the duct cross section at a fixed streamwise location had a maximum velocity on a ring at intermediate radius rather than at a point at the duct centre. This flow structure provided a powerful mechanism for flow entrainment, leading to an increase in effective jet spread rate which first became manifest 1.2 to 1.5 duct diameters downstream of the nozzle exit plane. In the case of the L_e/D_e = 2.25 ejector this permitted only a modest increase in ejector performance, although resonance was observed in that configuration. Of the geometries tested, it has already been noted that maximum benefit was evident at L_e/D_e = 4.25, and with much longer ducts the unsteady mixing mechanism added nothing to the level of entrainment available through random turbulent mixing.

The main potential applications of the phenomena described have high temperature primary jets. It is not presently clear how the higher gas velocities and density gradients involved might affect duct resonance, but there is no obvious reason why it should not occur, given appropriate conditions.

CONCLUSION

Pressure probing coupled with flow visualisation has helped to provide insight into the flow mixing mechanisms in high pressure ratio ejectors. An unsteady entrainment process has been described which results from natural duct resonance, and which greatly enhances the rate of mixing in the ejector. This might be exploited in certain specialised ejectors and combustors (and possibly avoided in others), but the effect of elevated primary jet temperature is not yet clear.

REFERENCES

Abdel-Fattah, A.M. (1985): Duct resonance in high pressure ratio thrust augmenting ejectors. Proc. 2nd Workshop on Wind Engineering and Industrial Aerodynamics, CSIRO, August 1985.

Fisher, S.A. (1980): Thrust augmenting ejectors for high pressure ratio propulsive jets. Proc. 7th Australasian Hydraulics and Fluid Mechanics Conference, Brisbane, August 1980.

Fisher, S.A.; Irvine, R.D. (1981): Air augmentation of rockets for low speed application. Proc. 5th International Symposium on Air Breathing Engines, Bangalore, February 1981.

Irvine, R.D. (1983): Static thrust augmentation of rocket motors by air entrainment. Weapons Systems Research Laboratory, WSRL-0332-TR, September 1983.

Quinn, W.R.; Pollard, A.; Marsters, G.F. (1985): Mean velocity and static pressure distributions in a three-dimensional turbulent free jet. AIAA Journal, Vol 23, No. 6, June 1985.